Time-Dependent Response of a Floating Flexible Plate to an Impulsively-Started Steadily Moving Load

W.S. Nugroho, K. Wang, R.J. Hosking,
and F. Milinazzo

DMS-784-IR August 1997

Time-dependent response of a floating flexible plate to an impulsively-started steadily moving load

By W.S. Nugroho[1]†, K. Wang[2], R.J. Hosking[2], AND F. Milinazzo[1]

[1]Department of Mathematics and Statistics, University of Victoria, Victoria, B.C., Canada V8W 3P4

[2]Department of Mathematics and Statistics, James Cook University of North Queensland, Townsville Q 4811, Australia

The time-dependent response of a floating flexible plate to an impulsively-started steadily moving load defines the time taken to approach a steady state deflexion due to the load, or indeed whether such a steady state is achieved at all. The asymptotic analysis for large time reported here, for both a concentrated point load and a uniformly distributed circular load, confirms that a steady state deflexion is achieved at both subcritical and supercritical load speeds. This analysis also predicts a logarithmically growing response near the critical speed corresponding to the minimum phase speed of the hybrid waves generated, but an eventual steady-state response when the load speed moves at the shallow water wave speed. These results are supported by numerical computation.

1. Introduction

Theory for the deflexion of a continuously-supported beam or plate due to a moving load is applicable to various transport systems. The beam or plate may represent a rail or road surface, an airport runway or a floating ice sheet in a cold region. The moving load might be a conventional vehicle, a landing aeroplane or a hovercraft. Moving loads on ice plates is the subject of a recent monograph (Squire *et al.*, 1996), where it is emphasised that the deflexion can be much greater when the load is moving than when it is stationary. Kerr (1983) pointed out that the minimum phase speed c_{min} of hybrid waves, largely determined by the flexural rigidity of the plate and the properties of the underlying foundation, coincided with a classical critical speed. Davys *et al.* (1985) subsequently noted that wave energy may accumulate beneath a load travelling at or near speeds coincident with both the group speed and the phase speed of generated waves. They also showed inter alia that gravity-dominated trailing waves may propagate away behind a localised load moving over a floating ice plate only if $V\cos\beta < \sqrt{gH}$, where V is the load speed and β is the angle that the normal to any wave crest makes with the direction in which the load is moving. The water wave speed $\sqrt{gH}$, where g is the gravitational acceleration and H is the depth of the underlying water, is thus another critical speed candidate. Leading shorter flexural waves correspond to wave numbers where the group speed exceeds the phase speed, and longer gravity-dominated waves to wave numbers where the reverse is the case.

† Present address: Fakultas Ilmu Komputer - Universitas Indonesia, Kampus UI-Depok Box 3442, Jakarta, Indonesia

In analysis for the response of a thin floating elastic plate to a steadily moving concentrated line load, on the implicit assumption that a steady state exists, Kheysin (1967) originally identified two critical speeds where the deflexion is theoretically infinite. Nevel (1970) subsequently analyzed the deflexion due to a steadily moving load uniformly distributed over a circular area, and inter alia noted that his integral for the deflexion directly beneath the load centre is unbounded at a particular load speed, so it emerged that such singularities were not due to load concentration or dimensionality.

Kheysin (1971) recognized that a time-dependent analysis might help explain the singular deflexion at critical speed. Thus he set out to examine whether or not the deflexion, evidently so dependent on the load speed, actually approaches a steady state – and if it does, to ascertain the time taken for transients to die out. He found that an impulsively-started concentrated line load produces a deflexion eventually growing in time as $t^{\frac{1}{2}}$ when $V = c_{min}$, consistent with continuous energy accumulation under the load at that speed (Davys *et al.* 1985). Schulkes & Sneyd (1988) provided a much more complete asymptotic analysis for an impulsively-started concentrated line load, confirming this $O(t^{1/2})$ growth when $V = c_{min}$ and showing inter alia that the deflexion also grows as $t^{\frac{1}{3}}$ when $V = \sqrt{gH}$ (as $t \to \infty$).

Steady wave patterns, originally derived by Davys *et al.* (1985) for a uniformly moving point load, have largely been reproduced for uniform rectangular load distributions by Milinazzo *et al.* (1995), with some small variations depending on load aspect ratio. However, they noted that whereas no bounded steady state is possible when $V = c_{min}$ (in the absence of dissipation), their steady state solution when $V = \sqrt{gH}$ appears bounded. Squire *et al.* (1996) nevertheless chose to refer to $\sqrt{gH}$ as "critical", pending the development of further relevant time-dependent analysis.

In this paper, we discuss the response of a floating flexible plate to an impulsively-started concentrated point load and an impulsively-started load uniformly distributed over a circular area, to investigate in particular whether the time-dependent deflexion at various load speeds V differs from that found by Schulkes & Sneyd (1988) for the one-dimensional case of a line load. The mathematical model we use is outlined in details in section 2.

2. Mathematical Model

We consider a thin elastic homogeneous plate of infinite extent, with thickness h and density ρ' floating on water of uniform depth H. The upper undisturbed water surface is at $z = 0$ and the seafloor is at $z = -H$, where the x, y plane coincides with the thin plate. The water density is denoted by ρ. If $f(x, y, t)$ denotes the moving load on the plate, then the linearized equation for the vertical plate deflexion $\eta(x, y, t)$ is (see Davys *et al.* 1985, Schulkes & Sneyd 1988)

$$D\left(\frac{\partial^2}{\partial x^2} + \frac{\partial^2}{\partial y^2}\right)^2 \eta + \rho' h \frac{\partial^2 \eta}{\partial t^2} = -\rho(\phi_t)_{y=0} - \rho g \eta - f(x, y, t) \qquad \text{for } -\infty < x, y < \infty \quad (2.1)$$

where the gravitational acceleration g is in the negative y direction and $\phi(x, y, z, t)$ represents the velocity potential for irrotational and incompressible flow in the water. The velocity potential thus satisfies the Laplace equation

$$\frac{\partial^2 \phi}{\partial x^2} + \frac{\partial^2 \phi}{\partial y^2} + \frac{\partial^2 \phi}{\partial z^2} = 0 \qquad -H < z < 0 \quad (2.2)$$

subject to the boundary conditions $\frac{\partial\phi}{\partial y}(x,y,-H,t)=0$ and the kinematic (non-cavitation) condition $\frac{\partial\phi}{\partial z}(x,y,0,t)=\frac{\partial\eta}{\partial t}|_{z=0}$. The flexural rigidity coefficient for a thin elastic plate is commonly given in terms of Young's modulus E and Poisson's ratio ν as

$$D=\frac{Eh^3}{12(1-\nu^2)}$$

although corrections can be made, such as to account theoretically for plate inhomogeneity for example (Kerr and Palmer 1972; Squire *et al.* 1996).

3. Time-dependent deflexion due to a point load

By considering a line load, Schulkes & Sneyd (1988) reduced the problem to one spatial dimension. In this paper, we consider a moving concentrated point load and then a uniformly distributed circular load in the next section, to discuss the time development of disturbances that may propagate in directions other than in the line of motion of the load.

Taking an impulsively-started point load subsequently travelling with uniform speed V in the positive x direction, we write $f(x,y,t)=P_0\delta(x-Vt)\delta(y)U(t)$ where P_0 is the load pressure per unit area, δ is the Dirac delta function and

$$U(t)=\begin{cases}0 & t\leq 0\\ 1 & t>0\end{cases}$$

is the Heaviside unit step function. Then taking the Fourier transform of (2.1) and (2.2) in x and y denoted by the hat superscript, we obtain

$$Dk^4\hat{\eta}+\rho g\hat{\eta}+\rho' h\hat{\eta}_{tt}+\rho\hat{\phi}_t(k,0,t)=-\frac{P_0}{2\pi}e^{-ik_1Vt} \tag{3.1}$$

for $t>0$, with

$$\hat{\phi}_{zz}-k^2\hat{\phi}=0 \tag{3.2}$$

$$\hat{\phi}_z(k,-H,t)=0 \qquad \hat{\phi}_z(k,0,t)=\hat{\eta}_t$$

where $k=\sqrt{k_1^2+k_2^2}$ is the wave number with Cartesian components (k_1,k_2), and the t and z subscripts indicates partial differentiation. Solving (3.2), substituting the result into (3.1) and using the initial conditions $(\hat{\eta})_{t=0}=0$, $(\hat{\eta}_t)_{t=0}=0$, we obtain

$$\left(\rho' h+\frac{\rho}{k}\coth(kH)\right)\hat{\eta}_{tt}+Dk^4\hat{\eta}+\rho g\hat{\eta}=-\frac{P_0}{2\pi}e^{-ik_1Vt}. \tag{3.3}$$

Given that we are interested in wavelengths much larger than the plate thickness h, we neglect the plate acceleration term with coefficient $\rho' h$ in (3.3). Upon solving the differential equation (3.3) we thus obtain

$$\hat{\eta}(k,t)=-\frac{P_0}{4\pi\rho}\,\frac{e^{-ik_1Vt}}{c(k)}\left[\frac{(1-e^{-i\Psi_1 t})}{\Psi_1}+\frac{(1-e^{i\Psi_2 t})}{\Psi_2}\right]\tanh(kH) \tag{3.4}$$

where $\Psi_1=kc-k_1V$ and $\Psi_2=kc+k_1V$ are suitable phase functions. The phase speed $c=\omega/k$, where ω is the angular frequency, is given by the dispersion relation (see also Figure 1)

$$c^2=\left(\frac{Dk^4}{\rho}+g\right)\frac{\tanh(kH)}{k}. \tag{3.5}$$

It is convenient to introduce the coordinate $X=x-Vt$ corresponding to a reference

frame moving with the load, so the expression for the plate deflexion obtained by the inverse Fourier transform is

$$\eta(X,y,t) = \\ -\frac{P_0}{8\pi^2\rho}\int_{-\infty}^{\infty}\int_{-\infty}^{\infty}\frac{\tanh(kH)}{c(k)}e^{i(k_1X+k_2y)}\left[\frac{(1-e^{-i\Psi_1 t})}{\Psi_1}+\frac{(1-e^{i\Psi_2 t})}{\Psi_2}\right]dk_1dk_2. \quad (3.6)$$

The phase speed $c(k)$ is positive for real k and the zeros of the denominators Ψ_1, Ψ_2 are also zeros of the respective numerators, so this expression is analytic in some neighbourhood of the real axis in the k_1k_2-plane. Some direct numerical computation using (3.6) is described later. To get asymptotic expansions for large time, we need only consider the term involving Ψ_1, since the other phase function Ψ_2 is monotonically increasing with k. We prefer to use an equivalent polar form for this purpose, however.

Using the polar coordinate transformation $X = r\cos\xi$, $y = r\sin\xi$, $k_1 = k\cos\theta$, $k_2 = k\sin\theta$, we re-express (3.6) as

$$\eta(r,\xi,t) = -\frac{P_0}{4\pi^2\rho}\Re\left(\int_0^{\infty}\int_{-\frac{\pi}{2}}^{\frac{\pi}{2}}\frac{\tanh(kH)}{c(k)}e^{ikr\cos(\theta-\xi)}\{\frac{1-e^{-ik(c-V\cos\theta)t}}{c-V\cos\theta}\right. \\ \left.+\frac{1-e^{ik(c+V\cos\theta)t}}{c+V\cos\theta}\}d\theta dk\right) \quad (3.7)$$

where $\Re(z)$ denotes the real part of z. An alternative expression for the deflexion in these polar coordinates is

$$\eta(r,\xi,t) = -\frac{P_0}{4\pi^2\rho}\int_0^{\infty}\int_{-\frac{\pi}{2}}^{\frac{\pi}{2}}\frac{k\tanh(kH)}{c(k)}\int_0^t\{\sin[kr\cos(\theta-\xi)+k(c+V\cos\theta)s] \\ -\sin[kr\cos(\theta-\xi)-k(c-V\cos\theta)s]\}dsd\theta dk \\ = -\frac{P_0}{2\pi\rho}\int_0^{\infty}\frac{k\tanh(kH)}{c(k)}\int_0^t J_0(kA)\sin(kcs)dsdk \quad (3.8)$$

where $A = \sqrt{(r\cos\xi+Vs)^2+r^2\sin^2\xi}$. Both (3.7) and (3.8) define the deflexion at any field point (r,ξ) in the plane of the flexible plate. For $t\to\infty$ and $V < c(k)$, (3.8) can be used to show that the maximum deflexion occurs at the concentrated point load (i.e. at $r = 0$ where $A = Vs$), as one might have anticipated in the absence of visco-elasticity (Takizawa 1988, Squire *et al.* 1996).

4. Local deflexion due to a distributed circular load

Let us now generalize the idea of Nevel (1970), to obtain the time-dependent deflexion under the centre of a load uniformly distributed over a circular area of radius R. Thus we introduce

$$\eta(t) = \int_0^R\int_0^{2\pi}\frac{\eta(r,\xi,t)}{\pi R^2}rdrd\xi,$$

so from equation (3.8) we have

$$\eta(t) = -\frac{P_0}{\pi\rho R}\int_0^\infty \frac{\tanh(kH)J_1(kR)}{c(k)}\int_0^t J_0(kVs)\sin(kcs)dsdk. \tag{4.1}$$

We note that the Bessel function $J_1(kR)$ in this result characterises the distributed load, in comparison with (3.8) for the concentrated point load.

The eventual evolved solution corresponds to setting $t = \infty$ in (4.1). Thus the fully evolved deflexion under the centre of the circular load is

$$\eta_\infty = -\frac{P_0}{\pi\rho R}\int_0^\infty \frac{\tanh(kH)J_1(kR)}{c(k)}\int_0^\infty \sin(kcs)J_0(kVs)dsdk$$

$$= -\frac{P_0}{\pi\rho R}\int_0^\infty \frac{\tanh(kH)J_1(kR)}{c(k)}\frac{U(c-V)}{\sqrt{k^2(c^2-V^2)}}dk;$$

and on introducing $a = kc^2/[g\tanh(kH)]$ and $b = kV^2/[g\tanh(kH)]$ we obtain the integral form derived by Nevel (1970):

$$\eta_\infty = -\frac{P_0}{\pi\rho R}\int_0^\infty \frac{J_1(kR)}{R}\frac{U(a-b)}{\sqrt{a(a-b)}}dk$$

$$= -\frac{P_0}{\pi\rho g\ell^2}\int_0^\infty \frac{J_1(\xi R/\ell)}{R/\ell}\frac{U(a-b)}{\sqrt{a(a-b)}}d\xi, \tag{4.2}$$

where U is the Heaviside unit step function introduced earlier and $\xi = kl$ is the nondimensional wave number (where $l = (D/\rho g)^{1/4}$ is a characteristic length). Non-zero contributions to the integral correspond to wave numbers k where $V < c(k)$, or equivalently $a > b$. Nevel noted that his integral in (4.2) is unbounded when $a = b$ and $da/d\xi = db/d\xi$, which in the deep water limit where $\tanh(kH)\approx 1$ corresponds to

$$V \approx 2(\frac{Dg^3}{27\rho})^{\frac{1}{2}},$$

the critical speed originally identified by Kheysin (1967) that is equivalent to $c_{\min}$.

We could numerically evaluate the deflexion given by (4.1) at various times t, to examine the evolution of the response for any given load speed V, including this critical speed. However, we are content to evaluate the integral in (4.1) asymptotically (as $t \to \infty$) in section 6, since the results obtained generally confirm the asymptotic analysis for the concentrated point load given in the next section.

5. Large time asymptotic analysis for the point load

Rather than asymptotically estimating the deflexion η for large t directly, we can often simplify our calculation by first differentiating with respect to t and estimating η_t instead, since the integrand is a continuous function of k and θ. We use the method of stationary phase (Nayfeh 1981, Lighthill 1978). Thus taking the derivative of (3.7) with respect to t, and retaining only the component which can contribute asymptotically due to points

of stationary phase, we consider

$$\eta_t(r,\xi,t) = \frac{P_0}{4\pi^2\rho}\Im\left(\int_0^\infty\int_{-\frac{\pi}{2}}^{\frac{\pi}{2}} \frac{k\ \tanh(kH)\ e^{ikr\cos(\theta-\xi)}}{c(k)} e^{-i\Psi t}d\theta dk\right) \tag{5.1}$$

where $\Psi = k(c - V\cos\theta)$ and $\Im(z)$ denotes the imaginary part of z. We can then integrate our asymptotic results for η_t, to get asymptotic estimates (as $t \to \infty$) for the deflexion η (Olver 1974).

Major contributions to the integral come from the neighbourhood of points of stationary phase. The stationary points of the double integral correspond to the (k,θ) pairs satisfying the two equations $\Psi_k(k,\theta) = c_g - V\cos\theta = 0$ and $\Psi_\theta(k,\theta) = kV\sin\theta = 0$ (with subscripts k and θ indicating partial differentiation), where $c_g = d\omega/dk$ denotes the group speed (Jones and Kline 1958, Cooke 1982).

Note that the stationary points depend crucially on the load speed V. Unless $k = 0$, they correspond to $\theta = 0$. In Figure 1 for example, we depict the zeros of Ψ_k (the two points of intersection k_A, k_B of the ordinate representing load speed V with the c_g-curve) when $c_{min} < V < \sqrt{gH}$. For all load speeds $V < \sqrt{gH}$, any stationary point is an interior point. For the load speed $V = \sqrt{gH}$, one stationary point is on the boundary (at the origin) and the other is an interior point. Considering the integration to be over the semi-infinite strip in the Cartesian (k,θ) plane where $|\theta| \le \frac{\pi}{2}$ and $k \ge 0$, when $k = 0$ we have $c_g = \sqrt{gH}$ so there are likewise stationary points on the boundary of this semi-infinite strip where $\theta = \pm\cos^{-1}(\sqrt{gH}/V)$, for $V > \sqrt{gH}$.

We now discuss the asymptotic contribution to the double integral in (5.1) from the neighbourhood of these stationary points for various load speeds V, in a fashion similar to the discussion given by Schulkes & Sneyd (1988) for the single integral in the case of a line load - cf. also Squire *et al.* (1996). Note that here it is the second or some higher order partial derivative in the phase function $\Psi = k(c - V\cos\theta)$ that is non-zero at the stationary point, in each case.

Case 1: Subcritical load speeds $V \le c_{gmin}$

Case 1a: $V < c_{gmin}$

If the load speed V is less than c_{gmin}, the minimum value of the group speed, then Ψ is a monotonically increasing function of k for any θ so there are no real stationary points. It follows that the deflexion decays exponentially with time, hence the steady state is approached relatively rapidly.

Case 1b: $V = c_{gmin}$

When $V = c_{gmin}$, there is only a single stationary point - viz. a point of inflexion relative to k, which we denote by $(k_s, 0)$. The Taylor expansion of the phase function Ψ in (5.1) about this point is thus

$$\Psi(k,\theta) = \Psi(k_s,0) + \frac{\Psi_{kkk}}{6}(k-k_s)^3 + \frac{\Psi_{\theta\theta k}}{2}\theta^2(k-k_s) + \frac{\Psi_{\theta\theta}}{2}\theta^2 + \cdots \tag{5.2}$$

where the partial derivatives are evaluated at the stationary point. We have that $\Psi_{kkk}(k_s,0) = (c_g)_{kk}(k_s,0) > 0$, $\Psi_{\theta\theta}(k_s,0) = k_sV > 0$, and $\Psi_{\theta\theta k}(k_s,0) = V > 0$, so introducing (5.2) into (5.1) gives

$$\eta_t(r,\xi,t) \approx$$
$$\frac{P_0}{4\pi^2\rho}\Im\left(\int_{k_s-\epsilon}^{k_s+\epsilon}\int_{-\epsilon}^{\epsilon}\frac{k\tanh(k_sH)\,e^{ik_sr\cos\xi}}{c(k_s)}\right.$$
$$\left.e^{-it(\Psi(k_s,0)+\frac{(c_g)_{kk}}{6}(k-k_s)^3+\frac{k_sV}{2}\theta^2+\frac{V}{2}(k-k_s)\theta^2)}\,d\theta dk\right)$$
$$=\frac{P_0}{2\pi^2\rho}\Im\left(\frac{\tanh(k_sH)\,e^{ik_sr\cos\xi}}{c(k_s)}\,e^{-it\Psi(k_s,0)}\right.$$
$$\left.\int_0^\infty k\,e^{-it\frac{(c_g)_{kk}}{6}(k-k_s)^3}\left(\int_0^\infty e^{-it\frac{V}{2}k\theta^2}d\theta\right)dk\right), \tag{5.3}$$

since $\epsilon > 0$ can be replaced by ∞ in the limit $t \to \infty$ and the integrand is even in θ. To the leading order term, the integral can be evaluated to yield

$$\eta_t(r,\xi,t) \approx$$
$$\frac{P_0\sqrt{3}}{6\sqrt{\pi^3\rho}}\frac{\sqrt{k_s}\tanh(k_sH)}{c(k_s)}\Gamma(\frac{1}{3})\,\Im\left(\frac{e^{ik_sr\cos\xi}e^{-i\frac{\pi}{4}}}{\sqrt{2V}\sqrt[3]{(c_g)_{kk}/6}}\,\frac{e^{-it\Psi(k_s,0)}}{t^{\frac{5}{6}}}\right). \tag{5.4}$$

We now integrate (5.4) from t to ∞ where $t > T$ and T is a sufficiently large fixed time (Olver 1974). Then after integrating by parts twice, we obtain (as $t \to \infty$)

$$\eta(r,\xi,t) \approx$$
$$\frac{P_0\sqrt{3}}{6\sqrt{\pi^3\rho}}\frac{\sqrt{k_s}\tanh(k_sH)}{c(k_s)}\Gamma(\frac{1}{3})\,\Im\left(\frac{e^{ik_sr\cos\xi}e^{-i\frac{\pi}{4}}}{\sqrt{2V}\sqrt[3]{(c_g)_{kk}/6}}\right.$$
$$\left.\left[\frac{e^{-it\Psi(k_s,0)}}{i\Psi(k_s,0)\,t^{\frac{5}{6}}}(1+\frac{5i}{6\Psi(k_s,0)t})-\frac{55}{36\Psi(k_s,0)^2}\int_t^\infty\frac{e^{-i\tau\Psi(k_s,0)}}{\tau^{\frac{11}{6}}}\,d\tau\right]\right). \tag{5.5}$$

For a concentrated line load at this load speed ($V = c_{gmin}$), Schulkes & Sneyd (1988) found that the most persistent transient decay is $t^{-\frac{1}{3}}$, whereas from (5.5) we conclude that transients due to a point load decay more quickly (as $t^{-\frac{5}{6}}$). Thus the deflexion produced by an impulsively-started concentrated point load tends rather more rapidly to the eventual steady state, by an additional factor $t^{-\frac{1}{2}}$.

Case 2: Subcritical load speeds $c_{gmin} < V < c_{min}$ and supercritical load speeds $c_{min} < V < \sqrt{gH}$

In these two load speed regimes, the two interior stationary points are denoted by $(k_A, 0)$ and $(k_B, 0)$, as illustrated in Figure 1 for the supercritical regime $c_{min} < V < \sqrt{gH}$. After expanding the integrand about the stationary points, the integral becomes

$$\eta_t(r,\xi,t) \approx$$
$$\frac{P_0}{4\pi^2\rho}\Im\left(\int_{k_A-\epsilon}^{k_A+\epsilon}\int_{-\epsilon}^{\epsilon}\frac{\tanh(k_AH)\ e^{ik_Ar\cos\xi}\ k_A}{c(k_A)}\ e^{-it(\Psi_A+\frac{\Psi_{kk}}{2}(k-k_A)^2+\frac{\Psi_{\theta\theta}}{2}\theta^2)}\ d\theta dk\right.$$
$$\left.+\int_{k_B-\epsilon}^{k_B+\epsilon}\int_{-\epsilon}^{\epsilon}\frac{\tanh(k_BH)\ e^{ik_Br\cos\xi}\ k_B}{c(k_B)}\ e^{-it(\Psi_B+\frac{\Psi_{kk}}{2}(k-k_B)^2+\frac{\Psi_{\theta\theta}}{2}\theta^2)}\ d\theta dk\right) \tag{5.6}$$

where the derivatives Ψ_{kk} and $\Psi_{\theta\theta}$ are evaluated at the stationary points. We observe that $\Psi_{kk}(k_B,0)>0$, $\Psi_{kk}(k_A,0)<0$, $\Psi_{\theta\theta}(k_A,0)>0$, $\Psi_{\theta\theta}(k_B,0)>0$ (and $\Psi_{k\theta}=\Psi_{\theta k}=0$ at both k_A and k_B). We also write Ψ_A to denote $\Psi(k_A,0)$ and Ψ_B to denote $\Psi(k_B,0)$.

Further evaluation as before yields

$$\eta_t(r,\xi,t) \approx$$
$$\frac{P_0}{4\pi^2\rho}\Im\left(\frac{\tanh(k_{s_1}H)\ e^{ik_Ar\cos\xi}\ k_A}{c(k_A)}e^{-it\Psi_A}\int_{-\infty}^{\infty}e^{-S^2}\frac{\sqrt{2}\ e^{i\frac{\pi}{4}}}{\sqrt{t}\sqrt{|\Psi_{kk}(k_A,0)|}}\ dS\right.$$
$$\left.\int_{-\infty}^{\infty}e^{-U^2}\ \frac{\sqrt{2}\ e^{-i\frac{\pi}{4}}}{\sqrt{t}\sqrt{\Psi_{\theta\theta}(k_A,0)}}\ dU\right)$$
$$+\frac{P_0}{4\pi^2\rho}\Im\left(\frac{\tanh(k_BH)\ e^{ik_Br\cos\xi}\ k_B}{c(k_B)}e^{-it\Psi_B}\int_{-\infty}^{\infty}e^{-S^2}\frac{\sqrt{2}\ e^{-i\frac{\pi}{4}}}{\sqrt{t}\sqrt{\Psi_{kk}(k_B,0)}}\ dS\right.$$
$$\left.\int_{-\infty}^{\infty}e^{-U^2}\ \frac{\sqrt{2}\ e^{-i\frac{\pi}{4}}}{\sqrt{t}\sqrt{\Psi_{\theta\theta}(k_B,0)}}\ dU\right)$$
$$=\frac{P_0}{2\pi\rho}\Im\left(\frac{\tanh(k_AH)\ e^{ik_Ar\cos\xi}\ k_A}{c(k_A)\sqrt{|\Psi_{kk}(k_A,0)|}\sqrt{\Psi_{\theta\theta}(k_A,0)}}\frac{e^{-it\Psi_A}}{t}\right)$$
$$-\frac{P_0}{2\pi\rho}\Re\left(\frac{\tanh(k_BH)\ e^{ik_Br\cos\xi}\ k_B}{c(k_B)\sqrt{\Psi_{kk}(k_B,0)}\sqrt{\Psi_{\theta\theta}(k_B,0)}}\frac{e^{-it\Psi_B}}{t}\right). \tag{5.7}$$

We again integrate from t to ∞ for $t>T$ where T is a sufficiently large fixed time, to obtain (after integrating by parts twice)

$$\eta(r,\xi,t) \approx$$
$$\frac{P_0}{2\pi\rho}\Im\left(\frac{\tanh(k_A H)\; e^{ik_A r\cos\xi}\; k_A}{c(k_A)\sqrt{|\Psi_{kk}(k_A,0)|}\sqrt{\Psi_{\theta\theta}(k_A,0)}}\left[\frac{e^{-it\Psi_A}}{i\Psi_A t}(1+\frac{i}{\Psi_A t})-\frac{2}{(\Psi_A)^2}\int_t^\infty \frac{e^{-i\tau\Psi_A}}{\tau^3}\,d\tau\right]\right)$$
$$-\frac{P_0}{2\pi\rho}\Re\left(\frac{\tanh(k_B H)\; e^{ik_B r\cos\xi}\; k_B}{c(k_B)\sqrt{\Psi_{kk}(k_B,0)}\sqrt{\Psi_{\theta\theta}(k_B,0)}}\left[\frac{e^{-it\Psi_B}}{i\Psi_B t}(1+\frac{i}{\Psi_B t})-\frac{2}{(\Psi_B)^2}\int_t^\infty \frac{e^{-i\tau\Psi_B}}{\tau^3}\,d\tau\right]\right). \tag{5.8}$$

Equation (5.8) shows that, in the two load speed regimes discussed in this section, the transients due to a concentrated point load decay as t^{-1}. This decay rate is again faster by a factor $t^{-1/2}$, compared with the case of a concentrated line load discussed by Schulkes & Sneyd (1988).

Case 3: Supercritical load speeds $V > \sqrt{gH}$

When the load speed V is greater than $\sqrt{gH}$, the stationary points near the origin are given by $(0, \pm\cos^{-1}(\sqrt{gH}/V))$. The third stationary point away from the origin is given by $(k_B, 0)$. At the stationary point $(0,\theta_s)$ where $\theta_s = \cos^{-1}(\sqrt{gH}/V)$, the non-zero derivatives up to the third order are $\Psi_{k\theta} = \Psi_{\theta k} = V\sin\theta_s$, $\Psi_{kkk} = (c_g)_{kk} < 0$, $\Psi_{\theta\theta k} = V\cos\theta_s$, so we get

$$\eta_t(r,\xi,t) \approx$$
$$\frac{P_0}{4\pi^2\rho}\Im\left(\int_0^\epsilon\int_{\theta_s-\epsilon}^{\theta_s+\epsilon}\frac{H}{c(0)}\,k^2\; e^{-it(\Psi_{k\theta}k(\theta-\theta_s)+\frac{\Psi_{\theta\theta k}}{2}k(\theta-\theta_s)^2+\frac{\Psi_{kkk}}{6}k^3)}\,d\theta dk\right)$$
$$+\frac{P_0}{4\pi^2\rho}\Im\left(\int_0^\epsilon\int_{-\theta_s-\epsilon}^{-\theta_s+\epsilon}\frac{H}{c(0)}\,k^2\; e^{-it(-\Psi_{k\theta}k(\theta+\theta_s)+\frac{\Psi_{\theta\theta k}}{2}k(\theta+\theta_s)^2+\frac{\Psi_{kkk}}{6}k^3)}\,d\theta dk\right)$$
$$+\frac{P_0}{4\pi^2\rho}\Im\left(\int_{k_B-\epsilon}^{k_B+\epsilon}\int_{-\epsilon}^{\epsilon}\frac{\tanh k_B H\; e^{ik_B r\cos\xi}\; k_B}{c(k_B)}e^{-it(\Psi_B+\frac{\Psi_{kk}}{2}(k-k_B)^2+\frac{\Psi_{\theta\theta}}{2}\theta^2)}d\theta dk\right). \tag{5.9}$$

In the limit $t\to\infty$, we again replace $\epsilon > 0$ by ∞, and evaluate the last integral in (5.9) as in the previous cases. The first two integrals in (5.9) can be combined and the inner θ integral then evaluated however, so we obtain

$$\eta_t(r,\xi,t) \approx$$
$$\frac{P_0}{\pi^{\frac{3}{2}}\rho}\Im\left(\frac{H}{c(0)}\frac{e^{-i\frac{\pi}{4}}}{\sqrt{2V\cos\theta_s}\sqrt{t}}\int_0^\infty k^{\frac{3}{2}}\, e^{it(\frac{V}{2}\cos\theta_s\tan^2(\theta_s)k-\frac{(c_g)_{kk}}{6}k^3)}dk\right)$$
$$-\frac{P_0}{2\pi\rho}\Re\left(\frac{\tanh k_BH\; e^{ik_Br\cos\xi}\; k_B}{c(k_B)\sqrt{\Psi_{kk}(k_B,0)}\;\sqrt{\Psi_{\theta\theta}(k_B,0)}}\frac{e^{-it\Psi_B}}{t}\right). \tag{5.10}$$

The integral in (5.10) can be estimated using the method of steepest descent (see Nugroho 1997 for details). Thus we obtain

$$\eta_t(r,\xi,t) \approx \frac{P_0}{2\pi\rho}\left(\frac{H\tan\theta_s}{c(0)|(c_g)_{kk}|}\frac{e^{-\frac{\tan^3(\theta_s)}{3}\sqrt{\frac{(V\cos\theta_s)^3}{|(c_g)_{kk}|}}t}}{t}\right)$$
$$-\frac{P_0}{2\pi\rho}\Re\left(\frac{\tanh k_BH\; e^{ik_Br\cos\xi}\; k_B}{c(k_B)\sqrt{\Psi_{kk}(k_B,0)}\;\sqrt{\Psi_{\theta\theta}(k_B,0)}}\frac{e^{-it\Psi_B}}{t}\right). \tag{5.11}$$

We again integrate from t to ∞ for $t > T$ where T is a sufficiently large fixed time, to obtain

$$\eta(r,\xi,t) \approx \frac{P_0}{2\pi\rho}\left(\frac{H\tan\theta_s}{c(0)\sqrt{|(c_g)_{kk}|}}\right.$$
$$\left[\frac{3e^{-\frac{(\tan\theta_s)^3}{3}\sqrt{\frac{(V\cos\theta_s)^3}{|(c_g)_{kk}|}}t}}{\sqrt{(V\cos\theta_s)^3}(\tan\theta_s)^3t}\left(1-\frac{3\sqrt{|(c_g)_{kk}|}}{\sqrt{(V\cos\theta_s)^3}(\tan\theta_s)^3t}\right)\right.$$
$$\left.\left.+\frac{18|(c_g)_{kk}|}{(V\cos\theta_s)^3(\tan\theta_s)^6}\int_t^\infty\frac{e^{-\frac{2}{3}\sqrt{\frac{(V\cos\theta_s)^3}{4|(c_g)_{kk}|}}(\tan\theta_s)^3\tau}}{\tau^3}d\tau\right]\right)$$
$$-\frac{P_0}{2\pi\rho}\Re\left(\frac{\tanh(k_BH)\; e^{ik_Br\cos\xi}\; k_B}{c(k_B)\sqrt{\Psi_{kk}(k_B,0)}\sqrt{\Psi_{\theta\theta}(k_B,0)}}\right.$$
$$\left.\left[\frac{e^{-it\Psi_B}}{i\Psi_Bt}(1+\frac{i}{\Psi_Bt})-\frac{2}{(\Psi_B)^2}\int_t^\infty\frac{e^{-i\tau\Psi_B}}{\tau^3}\,d\tau\right]\right). \tag{5.12}$$

Hence waves behind the load, which correspond to the contribution from the stationary points $(0,\pm\theta_s)$, disappear exponentially - i.e. much faster than the waves in front. The contribution from the stationary point $(k_B,0)$ defines the slower decay (as t^{-1}) of the transients associated with the leading shorter flexural waves. Once again, this decay is faster by a factor $t^{-1/2}$ compared with the case of a concentrated line load discussed by Schulkes & Sneyd (1988).

Case 4: Critical load speed $V = c_{min}$

For the critical load speed $V = c_{min}$, Schulkes & Sneyd (1988) showed that the deflexion grows in time as $t^{1/2}$, consistent with Kheysin (1971). For our double integral, at this load speed there are again two interior stationary points which we denote by $(k_A, 0)$ and $(k_{min}, 0)$, where k_{min} is the wave number at c_{min}. Since $\Psi(k_{min}, 0) = 0$, the Taylor expansion of the phase function $\Psi(k, \theta)$ about $k = k_{min}$ is

$$\Psi(k,\theta) = \frac{\Psi_{kk}}{2}(k - k_{min})^2 + \frac{\Psi_{\theta\theta}}{2}\theta^2 + \cdots,$$

and we note that $\Psi_{kk}(k_A, 0) < 0$, $\Psi_{kk}(k_{min}, 0) > 0$, $\Psi_{\theta\theta}(k_A, 0) > 0$, $\Psi_{\theta\theta}(k_{min}, 0) > 0$. Thus we obtain

$$\begin{aligned}\eta_t(r,\xi,t) \approx\ & \\ & \frac{P_0}{2\pi\rho}\Im\left(\frac{\tanh(k_A H)\, e^{ik_A r\cos\xi}\, k_A}{c(k_A)\sqrt{|\Psi_{kk}(k_A,0)|}\,\sqrt{\Psi_{\theta\theta}(k_A,0)}}\,\frac{e^{-it\Psi_A}}{t}\right) \\ & -\frac{P_0}{2\pi\rho}\Re\left(\frac{\tanh(k_{min}H)\, e^{ik_{min} r\cos\xi}\, k_{min}}{c(k_{min})\sqrt{\Psi_{kk}(k_{min},0)}\,\sqrt{\Psi_{\theta\theta}(k_{min},0)}}\,\frac{1}{t}\right). \end{aligned} \tag{5.13}$$

In this case, rather than integrating from t to ∞, we integrate from T to t where T is a sufficiently large fixed time, to get

$$\begin{aligned}\eta(r,\xi,t) \approx\ & \\ & \frac{P_0}{2\pi\rho}\Im\left(\frac{\tanh(k_A H)\, e^{ik_A r\cos\xi}\, k_A}{c(k_A)\sqrt{|\Psi_{kk}(k_A,0)|}\sqrt{\Psi_{\theta\theta}(k_A,0)}}\right. \\ & \left.\left[\frac{e^{-it\Psi_A}}{i\Psi_A t}\left(1+\frac{i}{\Psi_A t}\right)+\frac{e^{-iT\Psi_A}}{i\Psi_A T}\left(1+\frac{i}{\Psi_A T^2}\right)-\frac{2}{(\Psi_A)^2}\int_T^t \frac{e^{-i\tau\Psi_A}}{\tau^3}\,d\tau\right]\right) \\ & -\frac{P_0}{2\pi\rho}\Re\left(\frac{\tanh(k_{min}H)\, e^{ik_{min} r\cos\xi}\, k_{min}}{c(k_{min})\sqrt{\Psi_{kk}(k_{min},0)}\,\sqrt{\Psi_{\theta\theta}(k_{min},0)}}(\ln t - \ln T)\right). \end{aligned} \tag{5.14}$$

Thus the deflexion grows logarithmically in the limit $t \to \infty$. This is similar to the case of a concentrated line load, in that there is no steady solution at the critical load speed c_{min} (Kheysin 1971, Schulkes & Sneyd 1988), but the growth rate predicted for the concentrated point load is $O(\ln t)$ rather than $O(t^{1/2})$.

Case 5: Load speed $V = \sqrt{gH}$

As $V \to \sqrt{gH}$ from below, the stationary point $(k_A, 0)$ nearer to the origin $(0, 0)$ approaches it along $\theta = 0$, so in the limit $(k_A, 0) = (0, 0)$ is a boundary stationary point. When $V \to \sqrt{gH}$ from above, the two interior stationary points $(0, \pm\cos^{-1}\sqrt{gH}/V)$ merge into the origin. In passing, we recall that Schulkes & Sneyd (1988) noted that their relevant phase function, corresponding to setting $\theta = 0$ in our $\Psi = k(c - V\cos\theta)$, has a triple zero. At the origin, in our analysis we have that all partial derivatives of Ψ up to second order vanish and $\Psi_{kkk} = (c_g)_{kk} < 0$, $\Psi_{\theta\theta\theta} = -kV\sin\theta = 0$, $\Psi_{\theta\theta k} = V$, and $\Psi_{\theta kk} = 0$. Once again, introducing Taylor expansions into (5.1) we obtain

$$\eta_t(r,\xi,t) \approx$$
$$\frac{P_0}{2\pi^2\rho}\Im\left(\int_0^{\epsilon}\int_0^{\epsilon}\frac{H}{c(0)}\,k^2\,e^{-it(\frac{(c_g)_{kk}}{6}k^3+\frac{V}{2}k\theta^2)}\,d\theta dk\right)$$
$$+\frac{P_0}{4\pi^2\rho}\Im\left(\int_{k_B-\epsilon}^{k_B+\epsilon}\int_{-\epsilon}^{\epsilon}\frac{\tanh k_BH\;e^{ik_Br\cos\xi}\;k_B}{c(k_B)}e^{-it(\Psi_B+\frac{\Psi_{kk}}{2}(k-k_B)^2+\frac{\Psi_{\theta\theta}}{2}\theta^2)}\,d\theta dk\right), \tag{5.15}$$

where each of the derivatives is evaluated at the relevant stationary point. Further evaluation yields

$$\eta_t(r,\xi,t) \approx -\frac{P_0}{12\sqrt{\pi^3}\rho}\frac{H}{c(0)}\left(\frac{6}{|(c_g)_{kk}|}\right)^{\frac{5}{6}}\frac{\Gamma(\frac{5}{6})}{\sqrt{2V}}\frac{1}{t^{4/3}}$$
$$-\frac{P_0}{2\pi\rho}\Re\left(\frac{\tanh k_BH\;e^{ik_Br\cos\xi}\;k_B}{c(k_B)\sqrt{\Psi_{kk}(k_B,0)}\;\sqrt{\Psi_{\theta\theta}(k_B,0)}}\frac{e^{-it\Psi_B}}{t}\right).$$

We again integrate from t to ∞ where $t > T$ for sufficiently large fixed T, to obtain (as $t \to \infty$)

$$\eta(r,\xi,t) \approx \frac{P_0}{4\sqrt{\pi^3}\rho}\frac{H}{c(0)}\left(\frac{6}{|(c_g)_{kk}|}\right)^{\frac{5}{6}}\frac{\Gamma(\frac{5}{6})}{\sqrt{2V}}\frac{1}{t^{1/3}}$$
$$-\frac{P_0}{2\pi\rho}\Re\left(\frac{\tanh k_BH\;e^{ik_Br\cos\xi}\;k_B}{c(k_B)\sqrt{\Psi_{kk}(k_B,0)}\;\sqrt{\Psi_{\theta\theta}(k_B,0)}}\right.$$
$$\left.\left[\frac{e^{-it\Psi_B}}{i\Psi_Bt}(1+\frac{i}{\Psi_Bt})-\frac{2}{(\Psi_B)^2}\int_t^{\infty}\frac{e^{-i\tau\Psi_B}}{\tau^3}\,d\tau\right]\right). \tag{5.16}$$

The transient due to the stationary point $(0,0)$ decays as $t^{-\frac{1}{3}}$, whereas that due to the stationary point $(k_B,0)$ decays more quickly (as t^{-1}). This behaviour is in contrast to that for load speed $V=\sqrt{gH}$ in the case of a concentrated line load, where Schulkes & Sneyd (1988) found that the deflexion grows as $t^{\frac{1}{3}}$. A growing deflexion has not been reported when $V=\sqrt{gH}$ (see Takizawa 1985, Squire *et al.* 1985); and Schulkes & Sneyd (1988) observed "It is possible that $V=(gH)^{1/2}$ does not represent a critical speed for *two-dimensional sources*, because wave energy could radiate in all directions - not just along the line of motion". Our result shows that the time-dependent response is transient for a concentrated point load, so that the eventual deflexion at $V=\sqrt{gH}$ is steady state. This is consistent with the observation by Milinazzo *et al.* (1995), who found that the deflexion due to a uniformly moving distributed rectangular load is finite at the load speed $\sqrt{gH}$.

6. Large time asymptotic analysis for the distributed circular load

The time-dependent response for a uniformly distributed circular load is clarified by introducing the dimensionless time $t^*=kVt$, so that for the inner integral of (4.1) we

have

$$\int_0^{t^*} J_0(s)\sin(\lambda s)ds = \frac{1}{\pi}\int_0^{t^*}\int_0^{\pi}\cos(s\sin\theta)d\theta\sin(\lambda s)ds$$

$$= \Re\left(\frac{1}{2\pi}\int_{-\pi}^{\pi}\frac{1-e^{it^*(\lambda-\sin\theta)}}{\lambda-\sin\theta}d\theta\right) \tag{6.1}$$

where $\lambda = c(k)/V$. Noting that

$$\int_{-\pi}^{\pi}\frac{1}{\lambda-\sin\theta}d\theta = \begin{cases} 2\pi/\sqrt{\lambda^2-1}, & \lambda^2 > 1 \\ 0, & \lambda^2 \leq 1 \end{cases}$$

and returning to the original notation of (4.1), as $t \to \infty$ we therefore have

$$\int_0^t J_0(kVs)\sin(kcs)ds \approx \frac{U(c-V)}{\sqrt{k^2(c^2-V^2)}} - Re\{\frac{1}{\sqrt{2\pi kVt}}\frac{e^{-i[k(c-V)t+\frac{\pi}{4}]}}{k(c-V)}\}. \tag{6.2}$$

Substituting into (4.1), the time-independent component on the RHS of (6.2) produces the result (4.2) due to Nevel (1970) outlined in section 4. The time-dependent component on the RHS of (6.2) corresponds to the dominant time-dependent contribution (as $t \to \infty$) to the integral on the RHS of equation (6.1), arising from the neighbourhood of the point of stationary phase where $\cos\theta = 0$ (i.e. $\theta = \frac{\pi}{2}$). Thus from equation (4.1) we have the dominant time-dependent contribution to the deflexion (as $t \to \infty$), supplementing the evolved ($t = \infty$) solution (4.2) due to Nevel (1970), in the form:

$$\tilde{\eta}(t) = \frac{P_0}{\rho R}\frac{1}{\sqrt{2\pi^3 Vt}}Re\int_0^{\infty}\frac{\tanh(kH)J_1(kR)}{\sqrt{k}c(k)}\frac{e^{-i[k(c-V)t+\frac{\pi}{4}]}}{k(c-V)}dk. \tag{6.3}$$

The integral in equation (6.3) resembles the integral I_1 analysed by Schulkes & Sneyd (1988) for a line load, except that the range of integration is $(0,\infty)$ and the integrand has additional entries that are unimportant asymptotically -viz.$k^{-\frac{1}{2}}$ and the Bessel function $J_1(kR)$ corresponding to the uniformly distributed circular load of radius R. Accordingly, the time-dependence they found in the vicinity of a line load is moderated by the factor $t^{-\frac{1}{2}}$ outside the integral in equation (6.3). Thus we find the transient decay rates produced by the distributed load precisely the same as for the concentrated point load given in the previous section, for the respective subcritical and supercritical load speed regimes; viz.

- enhanced exponential decay if $V < c_{gmin}$, but $O(t^{-\frac{5}{6}})$ decay if $V = c_{gmin}$; and
- $O(t^{-1})$ decay if $c_{gmin} < V < c_{min}$ or $c_{min} < V < \sqrt{gH}$ or $V > \sqrt{gH}$.

Consequently, the deflexion produced by an impulsively-started uniformly distributed circular load likewise tends rather more rapidly to the evolved steady state (in this case Nevel's solution) due to the factor $t^{-\frac{1}{2}}$, in comparison with the transients in these regimes for a concentrated line load discussed by Schulkes & Sneyd (1988).

We can also deduce the time-dependent behaviour when the load speed V approaches the critical minimum phase speed c_{min} of hybrid waves, or the water wave speed $\sqrt{gH}$. Recall that for $c_{min} < V < \sqrt{gH}$ there are two points of stationary phase $k = k_A, k_B (0 < k_A < k_B)$ for the integral in (6.3), as illustrated in Figure 1, where the wave group speed coincides with the load speed ($c_g = V$). The dominant time-dependent contribution

is produced in the neighbourhood of k_A for the upper limiting speed $\sqrt{gH}$, and in the neighbourhood of k_B for the lower limiting speed c_{min}.

Our previous analytical approach was to first investigate the asymptotic behaviour (as $t\to\infty$) of the time-derivative of the deflexion and then deduce the corresponding asymptotic behaviour of the time-dependent component of the deflexion. Thus from equation (4.1) we have the exact time-derivative

$$\eta'(t) = -\frac{P_0}{\pi\rho R}\int_0^\infty \frac{\tanh(kH)J_1(kR)}{c(k)}J_0(kVt)\sin(kct)dk; \tag{6.4}$$

so invoking the well known asymptotic form

$$J_0(x) \;\approx\; \sqrt{\frac{2}{\pi x}}\cos(x-\frac{\pi}{4}), \qquad x\to\infty \tag{6.5}$$

for the Bessel function, we may first consider the behaviour of the asymptotic form for the time-derivative (as $t\to\infty$)

$$\eta'(t) = -\frac{P_0}{\rho R}\frac{1}{\sqrt{2\pi^3 Vt}}\int_0^\infty \frac{\tanh(kH)J_1(kR)}{\sqrt{k}c(k)}\sin[k(c-V)t+\frac{\pi}{4}]dk, \tag{6.6}$$

rather than the asymptotic form for the deflexion $\hat{\eta}(t)$ given by equation (6.3). In passing, we note that the asymptotic form in equation (6.6) also follows by differentiating the asymptotic form in equation (6.3), and it is an analytical advantage that the integral in equation (6.6) is regular at both critical load speeds (c_{min} and $\sqrt{gH}$).

When the load speed V approaches the water wave speed $\sqrt{gH}$ from below ($V\to\sqrt{gH}-$), the dominant contribution to the integral in equation (6.3) arises in the decreasing small but finite interval $(0,k_A)$, since the origin is then the limiting value of the first point of stationary phase k_A. In particular, on neglecting the plate acceleration term the dispersion equation for propagated waves is (c.f. Schulkes & Sneyd 1988; Squire *et al.* 1996)

$$c(k) = \sqrt{(\frac{Dk^2}{\rho}+g)\frac{1}{k}\tanh(kH)} \approx \sqrt{gH}(1-\frac{k^2H^2}{6}+\cdots), \tag{6.7}$$

so we have

$$c(k)-V \;\approx\; -\frac{k^2H^2}{6}V.$$

Hence when the load speed approaches the water wave speed from below ($V\to\sqrt{gH}-$), from equation (6.6) we find $\eta'(t) = O(t^{-\frac{1}{3}})$ as $t\to\infty$, so that $\tilde{\eta}(t) = O(t^{-\frac{1}{3}})$ as $t\to\infty$. Thus we find transients that eventually die away relatively slowly at the centre of a uniformly distributed circular load, in contrast to the $O(t^{\frac{1}{3}})$ growth in the deflexion found by Schulkes & Sneyd (1988) for an impulsively-started line load. Of greater interest is the case of time-dependence at the critical load speed $V = c_{min}$, the minimum phase speed of propagated waves. In this case we write

$$c(k) = c_{min} + \frac{1}{2}c''(k_{min})(k-k_{min})^2+\cdots,$$

where k_{min} denotes the wave number corresponding to the minimum phase speed c_{min} of generated waves. Thus as the load speed approaches this minimum phase speed from above ($V\to c_{min}+$), the dominant contribution to the integral in equation (6.6) arises

in a decreasing but significant small interval (k_{min}, k_B), where k_B is the second point of stationary phase. We therefore find $\eta'(t) = O(t^{-1})$ so that $\eta(t) = O(\ln t)$, as $t \to \infty$. Consequently, the deflexion due to an impulsively-started uniform circular load eventually grows logarithmically with time, in comparison with the $O(t^{\frac{1}{2}})$ growth as $t \to \infty$ found by Schulkes & Sneyd (1988) for an impulsively-started line load.

We can also evaluate the asymptotic time-dependent response (as $t \to \infty$) directly from (4.1). Thus first exchanging the order of the integration and then introducing the asymptotic form (6.5) for the Bessel function, we get

$$\eta(t) = -\frac{P_0}{\pi\rho R}\int_0^t\int_0^\infty \frac{\tanh(kH)J_1(kR)}{c(k)}\sin(kcs)J_0(kVs)dkds$$

$$\approx \eta(T) - \frac{P_0}{\sqrt{2\pi^3 V}R}\int_T^t \frac{1}{\sqrt{s}}\int_0^\infty \frac{\tanh(kH)J_1(kR)}{\sqrt{k}\,c(k)}$$

$$\left(\sin[k(c-V)s + \frac{\pi}{4}] + \sin[k(c+V)s - \frac{\pi}{4}]\right)dkds \qquad (6.8)$$

for sufficiently large fixed $T > 0$. Consequently, we consider the stationary points for the integral

$$I(t) = \Im\left(\int_0^\infty \frac{\tanh(kH)J_1(kR)}{\sqrt{k}c(k)}e^{ik(c-V)s}dk\right). \qquad (6.9)$$

Thus, when $V \to \sqrt{gH}$ from below and recalling (6.7), we have integral (6.9) represented asymptotically by

$$\int_0^\epsilon \frac{HR}{2V}k^{\frac{3}{2}}e^{-iH^2Vk^3s/6}dk = O(s^{-\frac{5}{6}}), \qquad (6.10)$$

and hence the transient component of the deflexion in (6.8) is

$$O(\int_T^t \frac{1}{\sqrt{s}}s^{-\frac{5}{6}}ds) = O(t^{-\frac{1}{3}}) \qquad (6.11)$$

as before. In the neighbourhood of $k = k_{min}$, a similar asymptotic evaluation of integral (6.9) produces a result of $O(s^{-\frac{1}{2}})$, so that the growth rate as $V \to c_{min}$ from above is confirmed as

$$O(\int_T^t \frac{1}{\sqrt{s}}s^{-\frac{1}{2}}ds) = O(\ln t). \qquad (6.12)$$

A similar analysis based upon (3.8) can be made for the concentrated point load, serving to emphasise that load concentration does not affect the time-dependence of the deflexion underneath the centre of the load, and that this time-dependence is to be seen at any field position where the disturbance is measurable.

7. Numerical Computation

To support the asymptotic results obtained in the previous sections, the double integral for the ice deflexion η in (3.6) was evaluated numerically using the Fast Fourier Transform (FFT), with from 512 to 4096 points in each direction. At the largest values of t, in some

cases it was necessary to use the greatest resolution in order to obtain acceptable results. In Figure 2 the effect on the numerical results of increasing the resolution from 512 by 512 to 2048 by 2048 can be seen. The curves $\eta(18, 18, t)$ obtained using the FFT become smoother as the resolution increases. The curve corresponding to the 2048 by 2048 grid is smooth up to about $t = 170$.

Since the asymptotic estimates for η are obtained by integrating η_t with respect to t, it is necessary to account for the constant that comes from the integration before a comparison with the numerical results can be made. This is achieved by adding a vertical offset to the asymptotic estimate so that the asymptotic and numerical estimates agree at a fixed point in time. The offset thus corresponds to the prior or steady state solution and as such depends on (X, y). Figures 2-7 compare the numerical and asymptotic estimates of the values of $\eta(X, y, t)$ for various values of (X, y). The parameter values are taken from Takizawa (1985). In all cases, the agreement is very good.

8. Conclusions

The steady state deflexion, caused by either a concentrated point load or a uniformly distributed circular load moving over a flexible floating plate, is generally reached more quickly in all load speed regimes than the time-dependent theory for a concentrated line load suggested. In the subcritical load speed regime $c_{gmin} \leq V < c_{min}$, and in the supercritical load speed regimes $c_{min} < V < \sqrt{gH}$ and $V > \sqrt{gH}$, the transient responses decay faster by a factor $t^{-1/2}$. Furthermore, a concentrated point load or a uniformly distributed circular load travelling at the critical speed c_{min} produces a deflexion that grows logarithmically with time (viz. $O(\ln t)$ rather than $O(t^{1/2})$ as $t \to \infty$); but when travelling at the shallow water wave speed $\sqrt{gH}$, there is a transient response that decays relatively slowly (viz. $O(t^{-1/3})$). All of these conclusions are independent of direction or distance from the load.

9. Acknowledgement

This research was supported, in part, by the Natural Sciences and Engineering Research Council of Canada under Grant OGP0009360-90 to F. Milinazzo. One of us (K. Wang) also acknowledges the award of an Overseas Postgraduate Research scholarship by the Commonwealth Government of Australia.

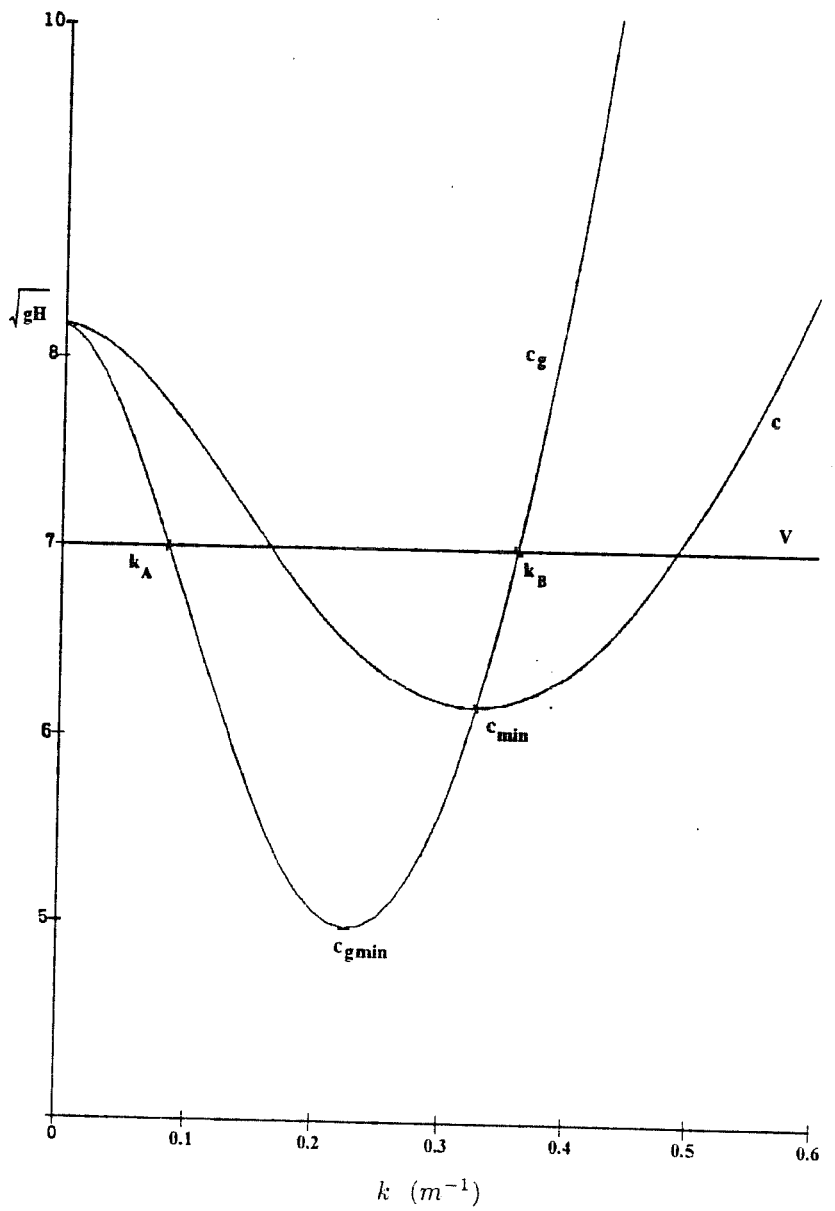

FIGURE 1. **Dispersion relation.** The parameters are $D = 2.5\text{x}10^5$, $\nu = \frac{1}{3}$, $h = 0.175$ m, $H = 6.8$ m, $g = 9.8$ ms^{-2}.

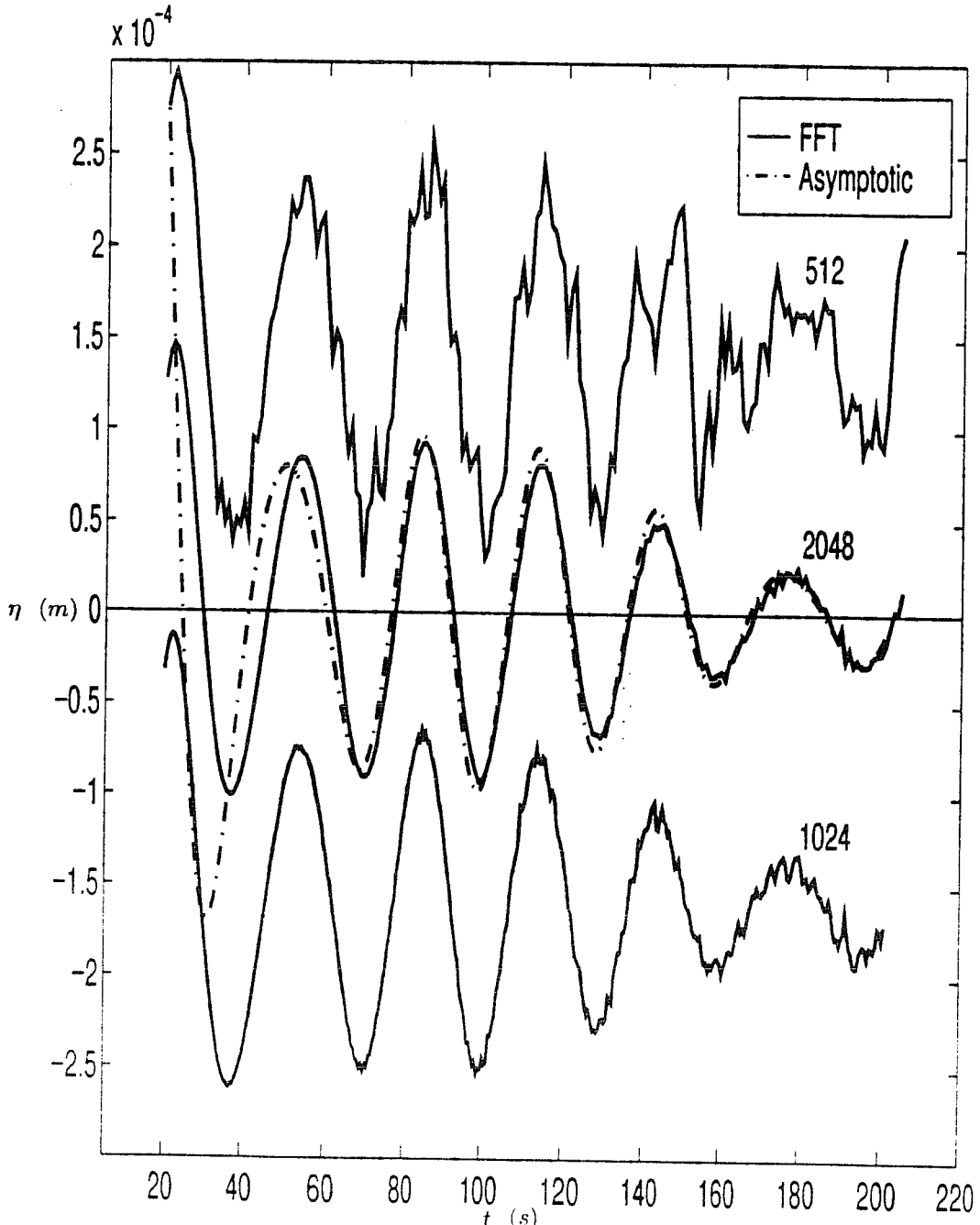

FIGURE 2. **Deflexion at a field point ahead of the load, at the subcritical load speed** $V = 5.5$ **ms**$^{-1}$. The figure shows the deflexion in meters against time in seconds at the observation point $X = 18.0$ m and $y = 18.0$ m. The results obtained using the Fast Fourier Transform (512 by 512 grid to 2048 by 2048 grid) are shown as the solid curves, whereas the result obtained using the asymptotic approximation (5.8) is shown as the dashed curve. The parameters are $D = 2.5\text{x}10^5$, $\nu = \frac{1}{3}$, $h = 0.175$ m, $H = 6.8$ m, $g = 9.8$ ms^{-2}, $V = 5.5$ ms^{-1}.

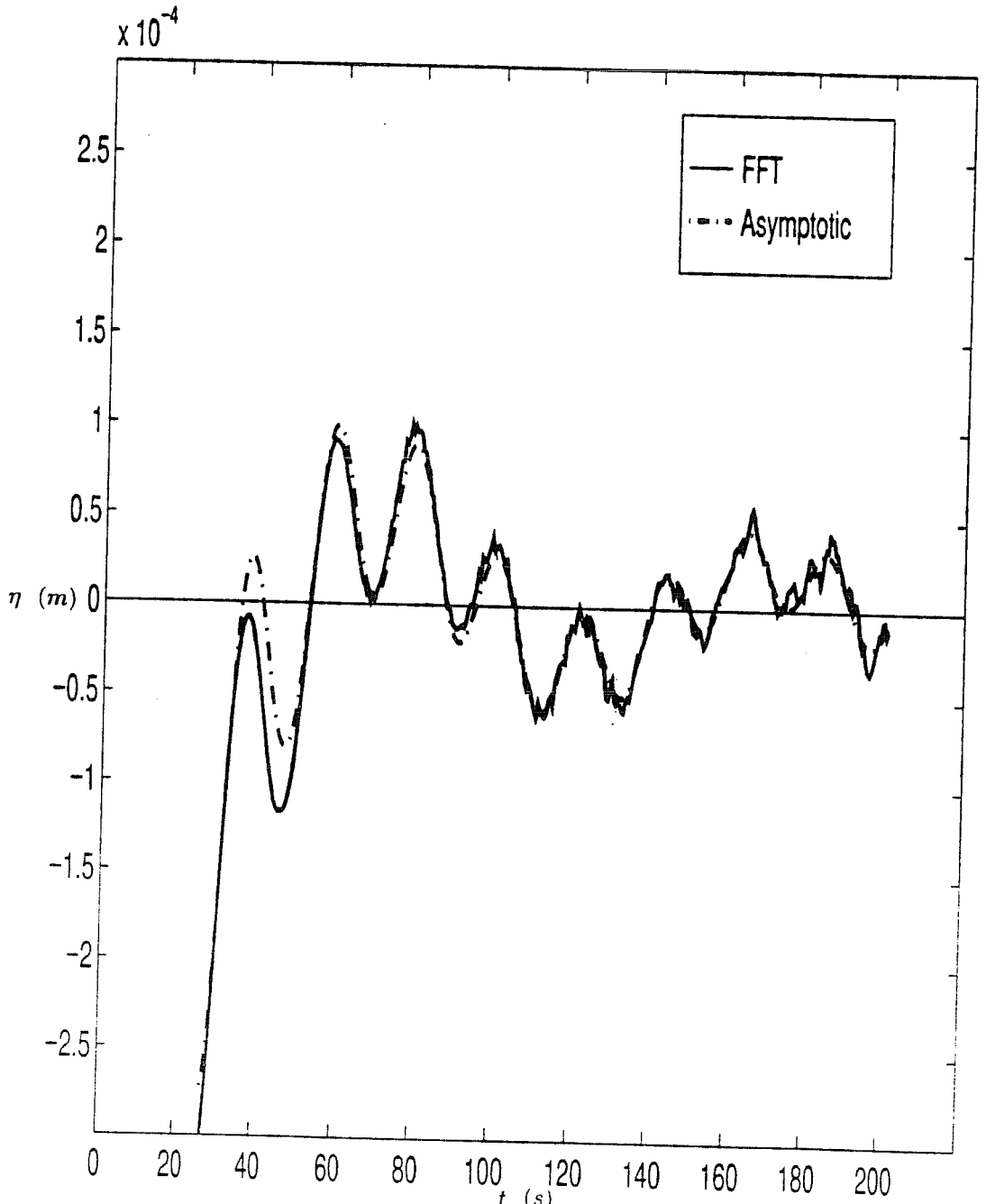

FIGURE 3. Deflexion at a field point behind the load, at the supercritical speed $V = 7.0$ ms^{-1}. The figure shows the deflexion in meters against time in seconds at the observation point $X = -18.0$ m and $y = 18.0$ m. The solid curve represents the result obtained using the Fast Fourier Transform (1024 by 1024 grid) and the dashed curve represents the result obtained using the asymptotic approximation (5.8). The parameters are $D = 2.5\text{x}10^5$, $\nu = \frac{1}{3}$, $h = 0.175$ m, $H = 6.8$ m, $g = 9.8$ ms^{-2}, $V = 7.0$ ms^{-1}.

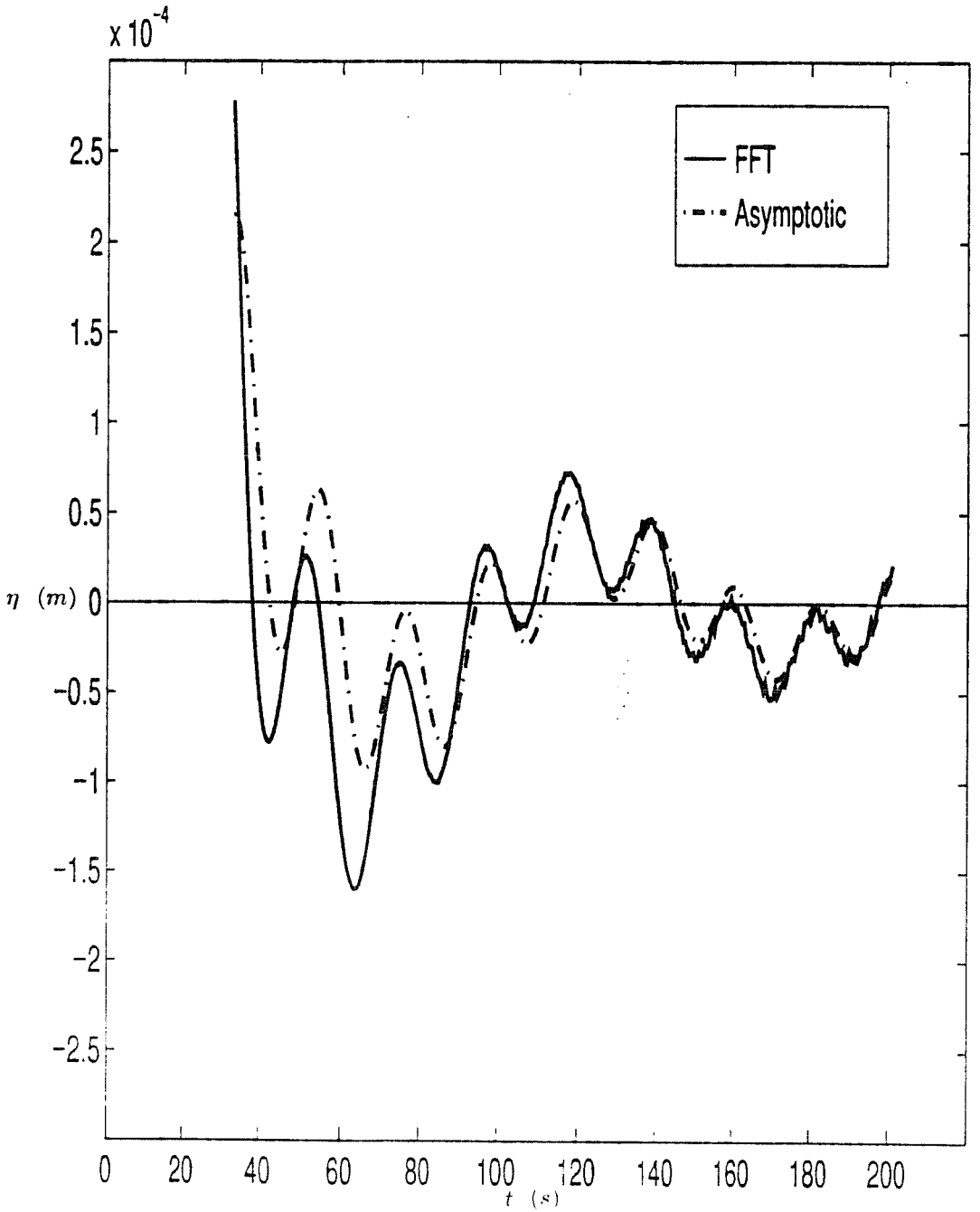

FIGURE 4. **Deflexion at a field point directly behind the load, at the supercritical load speed** $V = 7.0$ **ms**$^{-1}$. The figure shows the deflexion in meters against time in seconds at the observation point $X = -50.0$ m and $y = 0.0$ m. The result obtained using from the Fast Fourier Transform (2048 by 2048 grid) is shown as the solid curve and the result obtained using the asymptotic approximation (5.8) is shown as the dashed curve. The parameters are $D = 2.5\text{x}10^5$, $\nu = \frac{1}{3}$, $h = 0.175$ m, $H = 6.8$ m, $g = 9.8$ ms^{-2}, $V = 7.0$ ms^{-1}.

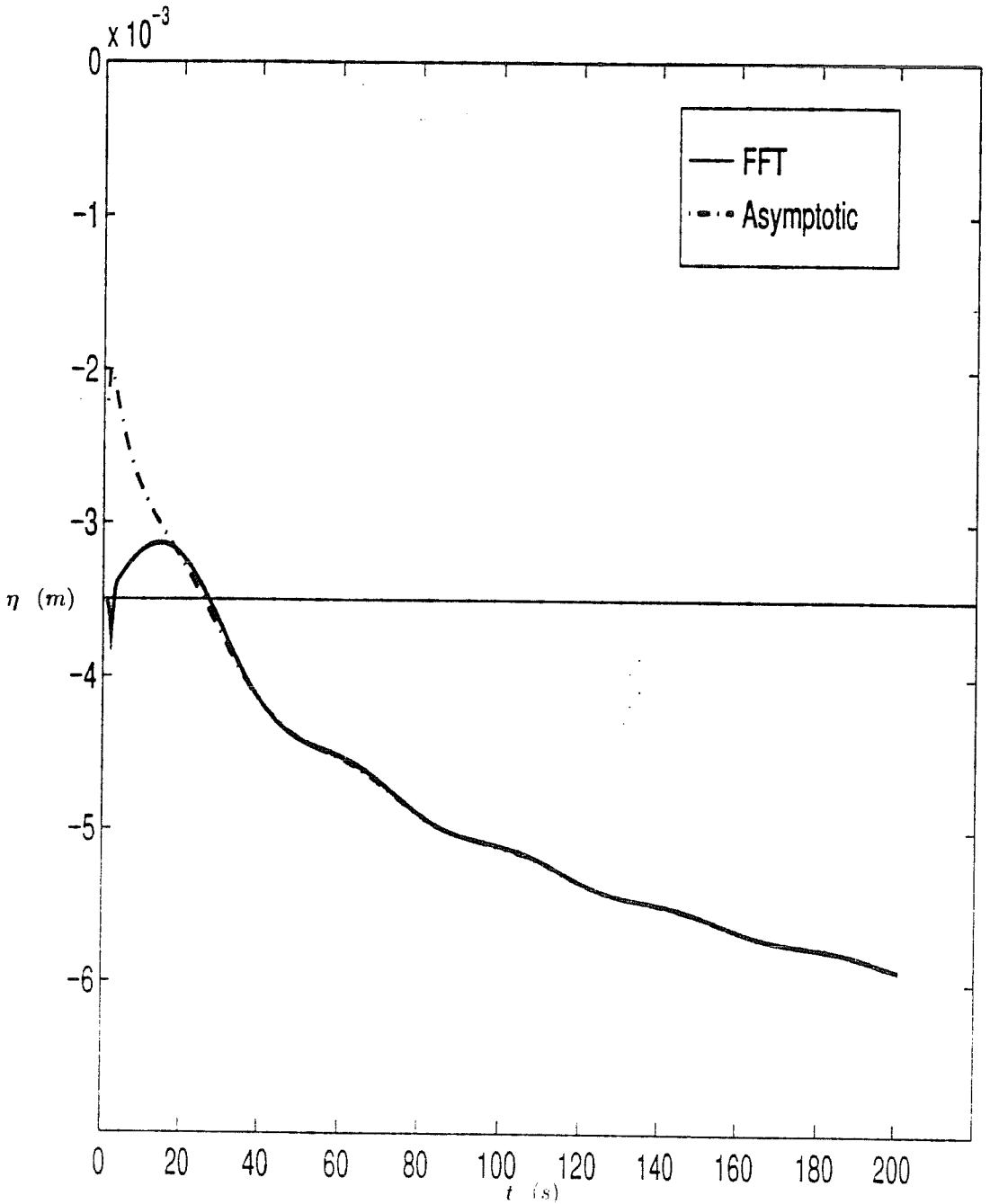

FIGURE 5. **Deflexion at a field point directly behind the load, at the critical load speed $V = 6.2$ ms^{-1} (c_{min}).** The figure shows the deflexion in meters against time in seconds at the observation point $X = -18.0$ m and $y = 0.0$ m. The result obtained using the Fast Fourier Transform (2048 by 2048 grid) is shown as the solid curve, and the result using the asymptotic approximation (5.14) is shown as the dashed curve. The parameters are $D = 2.5\text{x}10^5$, $\nu = \frac{1}{3}$, $h = 0.175$ m, $H = 6.8$ m, $g = 9.8$ ms^{-2}, $V = 6.2$ ms^{-1}.

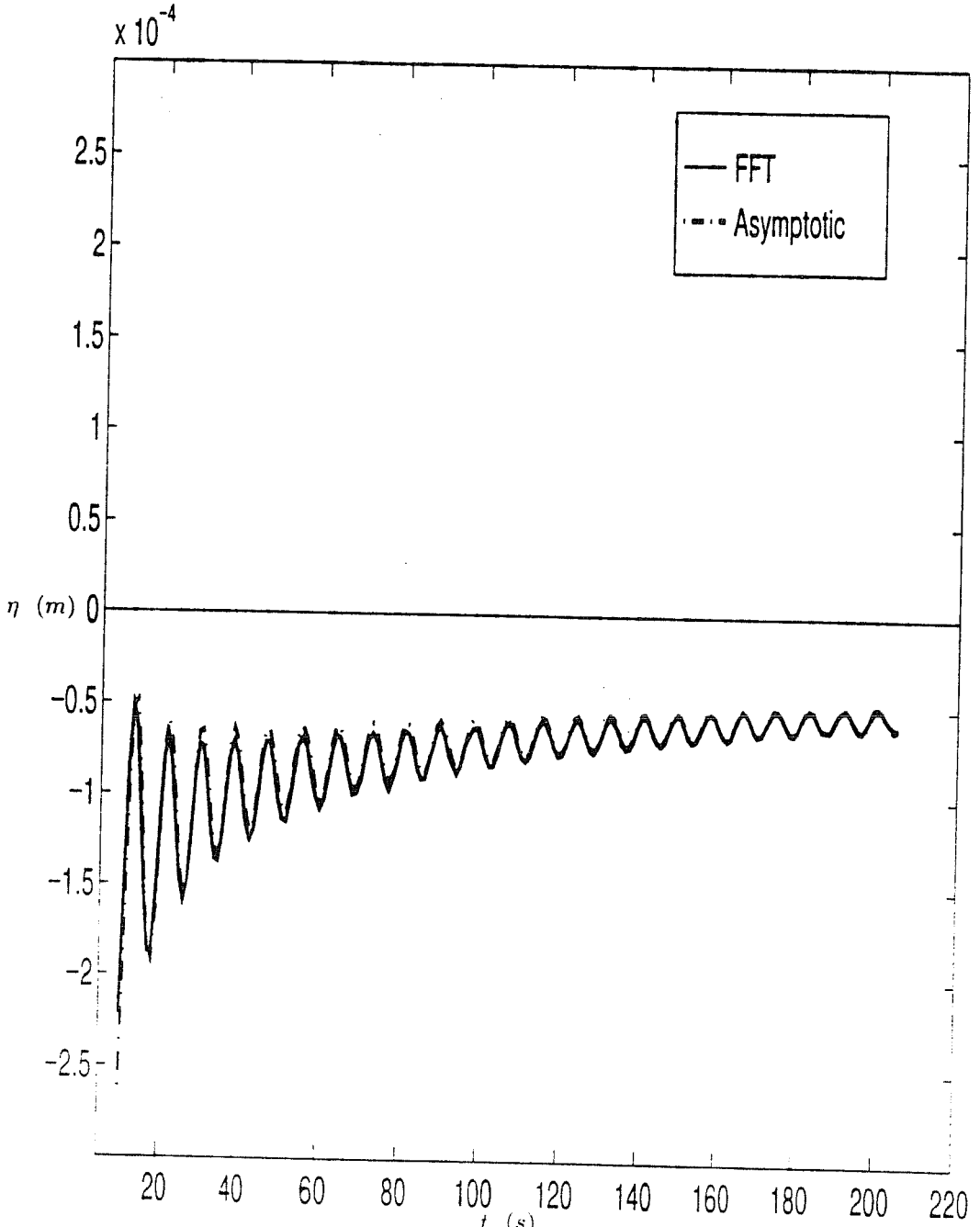

FIGURE 6. An illustration of the deflexion versus time at the load speed $\sqrt{gH}$. The figure shows the deflexion in meters against time in seconds at the observation point $X = 18.0$ m and $y = 0.0$ m. The solid curve represents the result obtained using the Fast Fourier Transform (4096 by 4096 grid), and the dashed curve represents the result obtained using the asymptotic approximation (5.16). The parameters are $D = 2.5\text{x}10^5$, $\nu = \frac{1}{3}$, $h = 0.175$ m, $H = 6.8$ m, $g = 9.8$ ms^{-2}, $V = 8.2$ ms^{-1}.

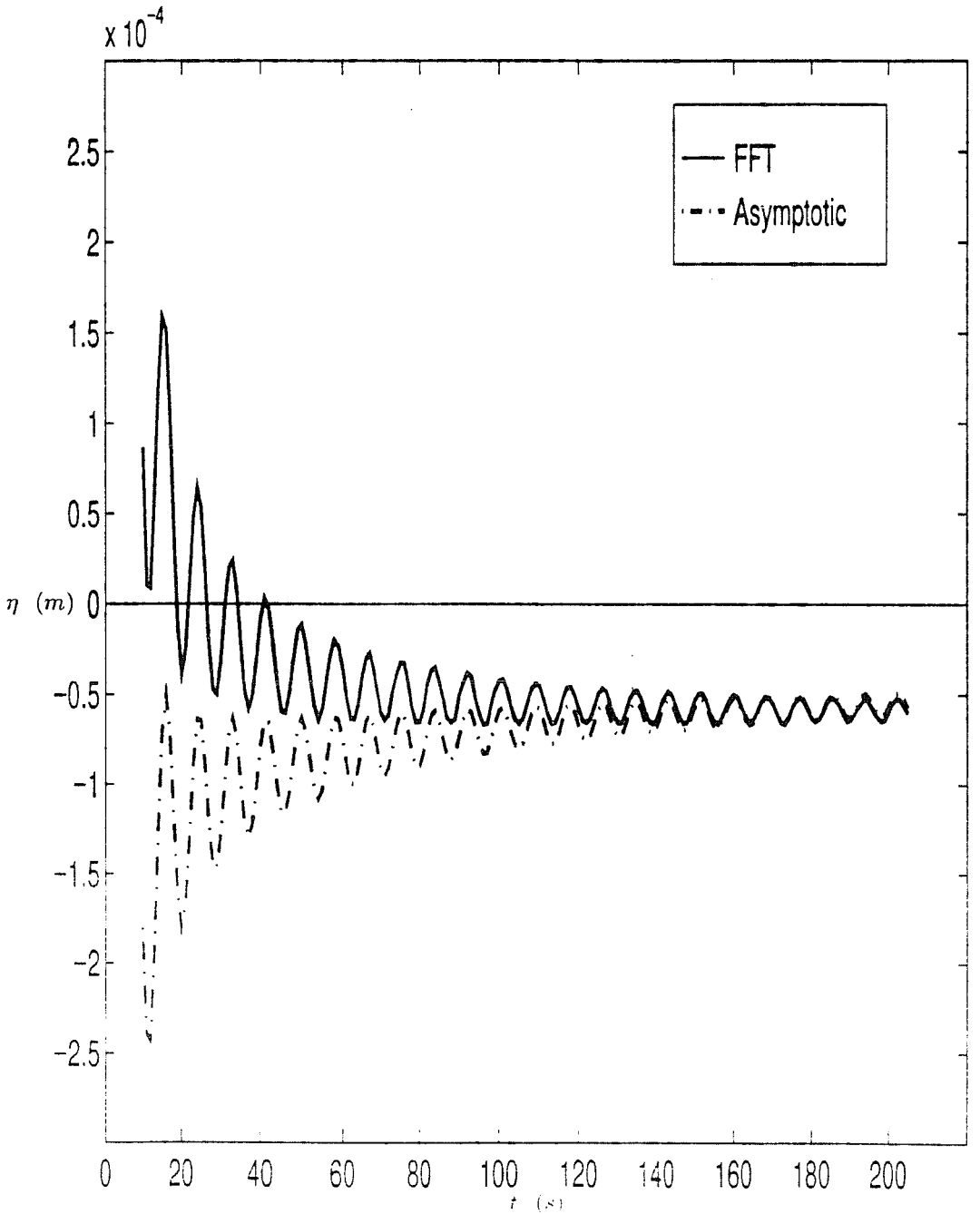

FIGURE 7. An illustration of the deflexion versus time at the load speed $\sqrt{gH}$. The figure shows the deflexion in meters against time in seconds at the observation point $X = -18.0$ m and $y = 0.0$ m. The solid curve represents the result obtained using the Fast Fourier Transform (4096 by 4096 grid), and the dashed curve represents the result obtained using the asymptotic approximation (5.16). The parameters are $D = 2.5\text{x}10^7$, $\nu = \frac{1}{3}$, $h = 0.175$ m, $H = 6.8$ m, $g = 9.8$ ms^{-2}, $V = 8.2$ ms^{-1}.

REFERENCES

COOKE, J.C. 1982 Stationary phase in two dimensions. *Journal of the Institute of Mathematics and Its Applications* **29**, 29–37.

DAVYS, J.W., HOSKING, R.J., & SNEYD, A.D. 1985 Waves due to a steadily moving source on a floating ice plate, *Journal of Fluid Mechanics* **158**. 269–287.

JONES, D.S. & KLINE, M. 1958 Asymptotic expansion of multiple integrals and the method of stationary phase, *Journal of Mathematical Physics* **37**. 1–28.

KERR, A.D. & PALMER, W.T. 1972 The Deformation and Stresses of Floating Ice Plates. *Acta Mechanica* **15**. 57-72.

KHEYSIN, Ye 1967 *Dynamics of the Ice Cover*. Gidrometeorologicheskoe Izdat-el'stvo. Leningrad. Technical Translation FSTC-HT-23-485-69. U.S. Army Foreign Science and Technology Center.

KHEYSIN, Ye 1971 Some unsteady-state problems in ice-cover dynamics, *Studies in Ice Physics and Ice Engineering* , ed. G.N. Yakovlev, Israel Program for Scientific Translations. 81–91.

LIGHTHILL, M.J. 1978 *Waves In Fluids*. Cambridge University Press.

MILINAZZO, F., M. SHINBROT. M., & EVANS, N.W. 1995 A Mathematical analysis of the steady response of floating ice to the uniform motion of a rectangular Load, *Journal of Fluid Mechanics* **287**. 173–197.

NAYFEH, A.H. 1981 *Introduction to Perturbation Techniques*, John Wiley & Sons.

NEVEL, D.E. 1970 Moving loads on a floating ice sheet. *Cold Regions Research and Engineering Laboratory Research Report 261*. Hanover, New Hampshire, U.S.A..

NUGROHO, W.S. 1997 *Waves generated by a load moving on an ice plate over water*. Ph.D. Dissertation, University of Victoria. Canada.

OLVER, F.W.J. 1974 *Introduction to Asymptotics and Special Functions*. Academic Press. Inc., New York.

SCHULKES, R.M.S.M. & SNEYD, A.D. 1988 Time-dependent response of floating ice plate to a steadily moving load, *Journal of Fluid Mechanics* **186**, 25–46.

SQUIRE, V.A., HOSKING, R.J., KERR, A.D. & LANGHORNE, P.J. 1996 *Moving Loads on Ice Plates*. Kluwer Academic Publishers.

SQUIRE, V.A., ROBINSON, W.H., HASKELL, T.G. & MOORE, S.C. 1985 Dynamic strain response of lake and sea ice to moving loads, *Cold Regions Science and Technology* **11**. 123–139.

TAKIZAWA, T. 1985 Deflection of a floating sea ice sheet induced by a moving load. *Cold Regions Science and Technology* **11**. 171–180.

TAKIZAWA, T. 1988 Response of a floating sea ice sheet to a steadily moving load, *Journal of Geophysical Research* **93**. 5100–5112.